Effect of metal nanoparticle concentration on localized surface plasmon mediated Förster resonant energy transfer

*Manuela Lunz(1)†, Xia Zhang(1), Valerie A. Gerard (2), Yurii K. Gun'ko (2), Vladimir Lesnyak (3), Nikolai Gaponik (4), Andrei S. Susha (5), Andrey L. Rogach (5), and A. Louise Bradley (1)**

(1) School of Physics and CRANN, Trinity College, Dublin 2, Ireland

(2) School of Chemistry and CRANN, Trinity College, Dublin 2, Ireland

(3) Istituto Italiano di Tecnologia, Via Morego 30, 16163 Genova, Italy

(4) Physical Chemistry, TU Dresden, Bergstrasse 66b, 01062 Dresden, Germany

(5) Department of Physics and Materials Science & Centre for Functional Photonics (CFP), City University of Hong Kong, Hong Kong, China

KEYWORDS

Quantum dots, Nanocrystals, Colloidal metal nanoparticles, Localised surface plasmons, Förster resonant energy transfer, Non-radiative energy transfer

ABSTRACT

The influence of gold nanoparticle concentration on signatures of localised surface plasmon mediated Förster resonant energy transfer is investigated in a quantum dot - gold nanoparticle sandwich structure. At lower gold nanoparticle concentrations localised surface plasmon mediated Förster resonant energy transfer enhancement of the acceptor emission is observed. At higher gold nanoparticle concentrations the acceptor emission is reduced, despite faster localised surface plasmon enhanced Förster resonant energy transfer rates being achieved. This is attributed to competition between localised surface plasmon mediated Förster resonant energy transfer and gold nanoparticle quenching effects.

INTRODUCTION

It has been predicted theoretically[1 - 3] that localized surface plasmons (LSP) supported by metal nanoparticles (NPs) can strongly enhance Förster resonant energy transfer (FRET)[4] – a dipole-dipole interaction mechanism – between donor and acceptor species. FRET has been proven to be a working mechanism for sensors,[5 - 7] energy harvesting structures[8, 9] and light emitting devices,[10 - 13] and thus, LSP mediated energy transfer could improve the efficiency and sensitivity of such FRET based devices. A few experimental demonstrations of LSP enhanced FRET have been reported over the past years.[14 – 23] In order to implement this effect in applications it is important to experimentally control LSP FRET. However, the analysis and investigation of the different parameters influencing this process is complicated by the fact that the LSPs do not only affect FRET between the donor and acceptor species, but also have an impact on the optical properties of the donors and acceptors directly, in form of PL quenching and enhancement.[24 – 35]

Due to their narrow and tunable emission bands,[36, 37] semiconductor quantum dots (QDs) have been widely used to investigate FRET[8, 38 – 42] as well as direct LSP quenching[27 – 30] and enhancement.[31 – 34] Furthermore, first experimental proofs of SP enhanced FRET have been reported in mixed donor-acceptor QD layers[17 – 19] as well as for separated QD structures.[20] These mostly focus on the evaluation of the improvement of FRET efficiencies, rates and / or Förster radii compared to QD FRET structures without metal NPs. From the work on the direct impact of LSPs on the optical properties of fluorophores, it is known that LSP quenching, as well as enhancement, effects depend crucially on the optical properties of the metal NPs and fluorophores as well as the separation between them.[25, 26, 29 – 32, 35] However, so far, only little has been reported on the impact of other important parameters, such as QD and metal NP concentration, metal NP-QD separations,

emission and absorption wavelengths of the QDs and metal NPs on the LSP FRET properties.

The focus of the work presented here lies on the influence of the gold NP concentration on the signatures of LSP mediated FRET in an acceptor QD-gold NP-donor QD sandwich structure. Varying the gold NP concentration reveals (i) LSP FRET enhancement of the acceptor emission at lower gold NP concentrations and (ii) gold NP quenching dominated acceptor emission at higher gold NP concentrations even though the FRET rate is further enhanced.

EXPERIMENTAL SECTION

Sandwich structures were prepared by a layer-by-layer (LbL) assembly technique.[43] The sandwich structures include an acceptor QD layer, an intermediate gold NP layer and a top donor QD monolayer, each separated by polyelectrolyte (PE) spacer layers. The PE layer thicknesses were validated by X-ray diffraction measurements. For comparison, reference structures comprised of single donor or acceptor monolayer, donor or acceptor monolayers on a gold NP monolayer as well as donor-acceptor bilayer structures were also investigated.

The donor and acceptor QD layers were prepared with negatively charged CdTe QDs, stabilized by thioglycolic acid in aqueous solution.[44] The donor QDs, with a diameter of 2.5 nm, have a central emission wavelength of 559 nm, while the acceptor QDs, with a diameter of 3.3 nm have an emission peak at 623 nm. The QD size as well as the concentration in the deposited monolayers were determined from absorption spectra,[44] measured with a double beam UV-Vis Spectrometer (Shimadzu UV-2401 PC). The gold NPs used were positively charged colloidal gold NPs, stabilized by 4-

dimethylaminopyridine (DMAP),[45] with an average diameter of 5.5 nm. Gold nanospheres of this dimension are suitable for LbL prepared structures with well-defined separations between the constituent layers.[20] The gold NP concentration in the layers was tuned by varying the immersion time from 1 to 20 minutes in a $1 \cdot 10^{-7}$ M gold NP solution and the gold NP layer concentration was determined from their absorption spectra with the corresponding extinction cross section.[46, 47]

All structures were prepared on quartz substrates covered with an initial PE buffer layer with an approximate thickness of 12 nm. The acceptor-gold NP separation and gold NP-donor separation were set to 12 nm and 3 nm, respectively, as this structure has been previously shown to exhibit clear signatures of LSP enhanced FRET.[20] A schematic of the sandwich structure is shown in Figure 1(a). The LSP resonance of the gold NPs, with an absorption peak at 532 nm, overlaps well with the donor photoluminescence (PL) emission and acceptor absorption peak, as can be seen in Figure S1 provided in the supporting information. Additional details on the sample preparation and the solution concentrations used for the deposition can be found elsewhere.[41, 48]

Signatures of LSP-FRET were characterized using PL, photoluminescence excitation (PLE) and time-resolved PL measurements. The QD PL and PLE spectra were recorded at room temperature with a Perkin-Elmer LS 55 fluorescence spectrometer using excitation provided by a pulsed Xenon lamp. For the PL spectra an excitation wavelength of 400 nm was used. Time-resolved donor PL decays were measured using a 500 nm broad band-filter with a full width at half maximum of approximately (70 ± 5) nm, to record the emission from the donor QDs only. The decay signal was recorded using a x40 objective lens over an area of 80 x 80 μm^2 (150 x 150 pixels) with a PicoQuant Microtime 200 time-resolved confocal microscope with 150 ps time resolution. Picosecond excitation pulses at a

wavelength of 470 nm were provided by a LDH-480 laser head, controlled by a PDL-800B driver (PicoQuant), with an average power of 16 nW. Typically a repetition rate of 10 MHz and an integration time of 4 ms per pixel were used. All PL spectra and decay measurements were repeated at more than one position on each sample to confirm sample uniformity, as well as reproducible excitation and collection conditions.

RESULTS AND DISCUSSION

As mentioned above, the investigation of the effect of LSPs on FRET between QDs is complex in that the gold NPs not only mediate energy transfer over a larger separation,[20] but they also have a direct influence on the QD PL which depends on the QD-gold NP separation and gold NP concentration.[25, 26, 29 – 33] For the QDs and gold NPs used in this study only PL quenching was observed for bilayer structures comprised of a QD monolayer on a gold NP layer, for both the donor or acceptor QDs (as can be seen from the PL ratios presented in Figures 2 and the lifetime data shown in Figure 3, which will be discussed in more detail later). Characterization of the LSP FRET sandwich structure after the deposition of each constituent layer revealed that at an acceptor-gold NP separation of 12 nm there is no emission visible from the acceptor QD monolayer. The acceptor emission is only recovered after the donor QD layer has been deposited, providing evidence for LSP FRET.[20] This structure is well suited to investigation of LSP FRET as the signatures such as enhancement of the acceptor emission can be clearly identified with LSP FRET and not LSP emission enhancement effects.

Typical spectra for the acceptor-gold NP-donor sandwich structure with different gold NP concentrations can be seen in Fig. 1(a). The spectrum of a reference bilayer structure without gold NPs and a layer separation of 21 nm is also included. For the reference

bilayer a separation of 21 nm was selected as it corresponds to the total separation between the donor and acceptor layers in the sandwich structure. As can be seen, for the lowest gold NP concentration investigated (blue line), the acceptor emission is increased relative to that of the reference structure without gold NPs (open squares), whereas the donor emission is slightly decreased. With increasing gold NP concentration, both the donor and acceptor QD emission are decreasing.

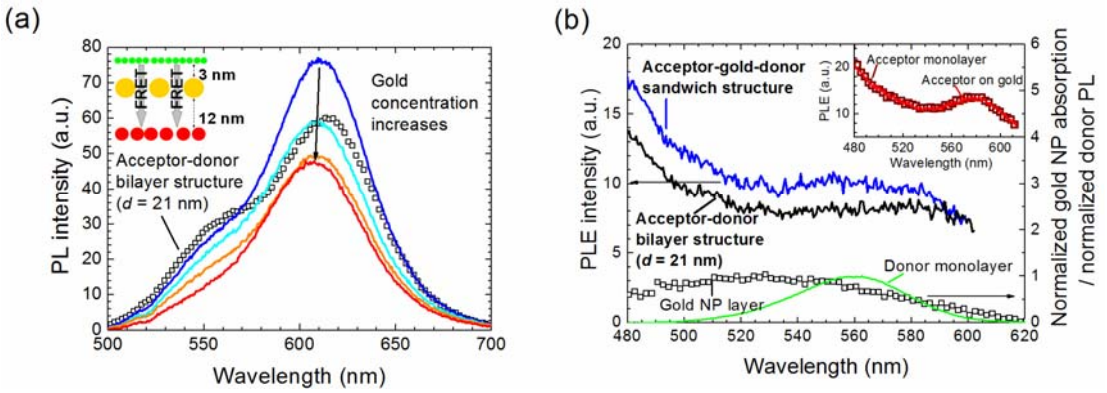

Figure 1. (a) Emission spectra of acceptor-gold-donor sandwich structures with different gold NP concentrations as well as a reference bilayer structure without gold NPs. A schematic of the sandwich structure is shown in the top left corner. (b) Acceptor PLE spectra of an acceptor-donor bilayer structure (separation 21 nm, black line) and the full sandwich structure with an acceptor-gold separation of 12 nm, a gold-donor separation of 3 nm and a gold NP concentration of $c_{Au} = 0.026 \cdot 10^{17}\, m^{-2}$ (blue line). For reference the normalized gold NP absorption (open black squares) and donor PL emission (green line) are also included. The inset shows the acceptor PLE spectra of an acceptor monolayer (open, dark red squares) and an acceptor monolayer on a gold NP layer (separation 12 nm, red line).

Further evidence for LSP FRET can be seen in the PLE spectra of a sandwich structure (blue line) with a low gold concentration shown in Figure 1(b) in comparison with a similar bilayer structure without gold NPs (black line). There is no difference in the acceptor PLE spectra without donor QDs (included in the inset of Fig. 1(b)), indicating that there is no direct acceptor enhancement by layers with a low gold NP concentration at this gold NP-acceptor separation. The PLE spectrum of the sandwich structure, however, shows higher emission than the bilayer structure without gold NPs and an additional feature between 530 to 590nm. This feature appears at wavelengths where the donor emission and the LSP absorption peak (also included in the Figure) overlap. This is evidence of LSP mediated energy transfer from the donors to the acceptors at acceptor-donor separations at which normally no energy transfer is observed.

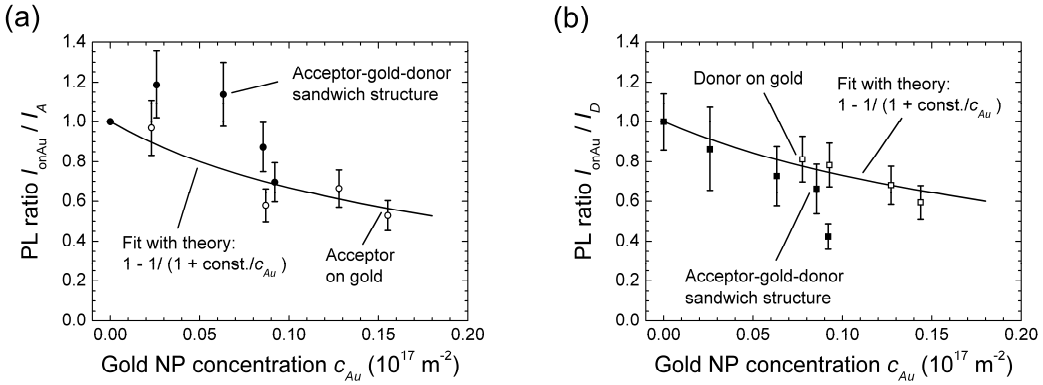

Figure 2. (a) PL ratio of the acceptor emission in a sandwich structure, $I_{Acc,Sandwich} / I_{Acc,BL}$, and an acceptor on gold structure, $I_{Acc,on\,gold} / I_{Acc,ML}$, as a function of the gold NP concentration. The line represents a fit of the PL quenching with theory for the acceptor on gold structure. (b) Gold NP concentration dependence of the PL ratio of the donor emission in a sandwich structure, $I_{Don,Sandwich} / I_{Don,BL}$, and a donor on gold

structure, $I_{Don,on\,gold}/I_{Don,ML}$. The line represents a fit of the donor PL quenching on gold with theory.

For a more quantitative analysis, the changes in the donor and acceptor emission properties are compared to those of only donor or acceptor QD monolayers on gold NP layers. To correct for variations due to small differences in the QD concentration, the relative emission with respect to structures with the same QD concentration but without gold NPs, i.e. a donor-acceptor bilayer structure or pure QD monolayer, was calculated. The PL ratio for the acceptor emission in the sandwich structure relative to the bilayer structure with no gold NP layer, $I_{Acc,Sandwich}/I_{Acc,BL}$, is shown as a function of the gold NP concentration in Fig. 2(a). Also plotted is the PL ratio for the acceptor on gold structures relative to an acceptor monolayer, $I_{Acc,on\,gold}/I_{Acc,ML}$. The trend measured for the acceptor on gold structures is fitted with a theory for non-radiative energy transfer between two planes – the fit with a FRET or nanometal surface energy transfer model results in the same concentration dependence.[30] In particular, even values larger than 1 are observed for the two lowest gold NP concentrations investigated, corresponding to an absolute acceptor emission increase compared to bilayer structures with the same acceptor concentration but no gold NPs. The increase of the acceptor emission in the sandwich structure over that of the acceptor on gold structures decreases, however, with increasing gold NP concentration, reflecting the competition of two effects: the acceptor emission enhancement due to LSP FRET and the direct acceptor QD emission quenching by the gold NPs.

This competition is further evidenced in the LSP FRET enhancement of the gold quenched acceptor PL, ΔI_{Acc-Au}, summarized in Table 1. These values have been

calculated from the PL ratios for the sandwich structure relative to the bilayer structure, $I_{Acc,Sandwich}/I_{Acc,BL}$, shown in Fig 2(a) and the values of the PL ratio of the acceptor on gold structure relative to the acceptor monolayer, $I_{Acc,on\,gold}/I_{Acc,ML}$, at the same gold NP concentration which were obtained from the fit included in Fig. 2(a). As can be seen, the LSP FRET enhancement of the gold quenched acceptor PL is highest for the second lowest gold NP concentration investigated and decreases with further increase of the gold NP concentration. This shows that at higher gold NP concentrations the direct quenching by the gold NPs dominates the acceptor emission.

The donor PL ratio, plotted as a function of the gold NP concentration in Fig. 2(b), shows a trend opposite to that of the acceptor PL ratio. The donor emission in the sandwich structure is always lower than that expected for a donor on gold structure with the same gold NP concentration. The trends of increased acceptor emission and the decreased donor emission are again clear evidence for LSP mediated FRET from the donor to the acceptor QDs in the sandwich structure. Furthermore, the difference between the donor PL ratio emission in the sandwich structure and that for the donor on gold is seen to increase with increasing gold NP concentration indicating that FRET to the acceptor QDs via the gold NPs is increasing.

The donor PL decay properties are an important signature of FRET and can be used to further evaluate the LSP FRET. The main impact of LSP enhanced FRET is seen in the short lifetime component in this structure for these particular QDs.[20] Examples of the measured PL decays are given in the inset of Fig. 3. Firstly, it can be noted that the donor PL decay for the sandwich structure is faster than for the donor on gold structure with similar donor and gold NP concentrations. It can also be seen that the PL decay lifetime shortens with increasing gold NP concentration in the sandwich structure. The gold NP

concentration dependence of the relative donor lifetime for the sandwich, $\tau_{Don,Sandwich}/\tau_{Don,BL}$, and donor on gold structures, $\tau_{Don,on\ gold}/\tau_{Don,ML}$, is shown in Fig. 3. The lifetimes are given as relative values with respect to donor lifetimes in donor monolayers with the same QD concentration in order to correct for differences arising from variations in the donor concentration.[48] The measured lifetimes for all sandwich and reference structures are given in the supplementary information.

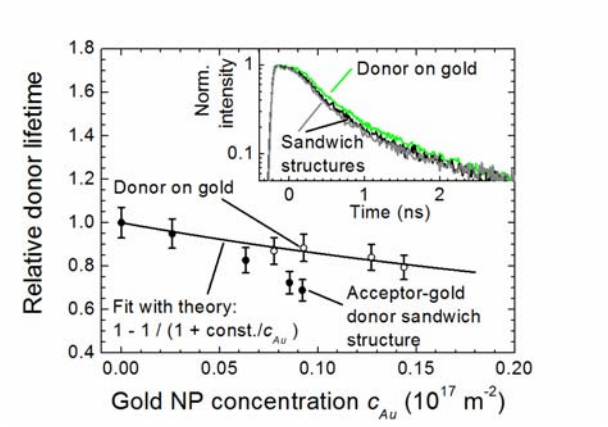

Figure 3. Relative donor lifetime in a sandwich structure, $\tau_{Don,Sandwich}/\tau_{Don,BL}$, and a donor on gold structure, $\tau_{Don,on\ gold}/\tau_{Don,ML}$, calculated as a ratio with the respective donor lifetimes in a donor QD monolayer with the same QD concentration. The line indicates a fit of the lifetimes in a donor-gold structure with theory for quenching by non-radiative energy transfer. Shown in the inset is a close-up of the first 3 ns of the donor PL decay in two sandwich structures (grey and black line) with different gold NP concentrations (black line: $c_{Au} = 0.086 \cdot 10^{17}$ m^{-2}, grey line: $c_{Au} = 0.092 \cdot 10^{17}$ m^{-2}) as well as for a donor on gold structure with similar donor and gold NP concentrations (green line).

In line with increasing donor emission quenching, the decrease of the short component of the donor PL lifetime - with respect to the lifetime determined for the donor on gold

structures without acceptor QDs - is stronger with increasing gold NP concentration. Comparing the short donor lifetime component in the sandwich structures with the values of the donor lifetime for a donor on gold structure at the same gold NP concentration, taken from the fit with theory for quenching by non-radiative energy transfer (line), shows that the FRET rate, $k_{FRET-LSP}$, (also given in Table 1) increases from $(6 \pm 2\,\mathrm{ns})^{-1}$ to $(2.1 \pm 0.3\,\mathrm{ns})^{-1}$ with increasing gold NP concentration from $c_{Au} = 0.063 \cdot 10^{17}\ m^{-2}$ to $0.092 \cdot 10^{17}\ m^{-2}$. At the lowest NP gold concentration investigated, $c_{Au} = 0.026 \cdot 10^{17}\ m^{-2}$, the difference between the donor lifetime of the sandwich structure and that from the fit to the donor on gold data is within the error on the lifetime measurements, and consequently this sample is not included in the below discussion of the FRET rate. However, the smaller lifetime difference at the lower concentration further demonstrates that the FRET rate is even slower at lower concentrations. The error on the calculated FRET rate reduces with increasing Au NP concentration and a clear trend of increasing LSP FRET rate with increasing Au NP concentration over the range studied is observed, in agreement with the shortening of the PL decays as shown in Fig. 3.

Several theoretical and experimental reports in the literature have shown that energy transfer between QDs can be well described by the theory of FRET between two dipoles, despite the relatively large size of the QDs.[40,41,48,49] In comparisons of experiment and theory the CdTe QDs were approximated as spheres, and the QD radii were used in the calculation of the centre-to centre separations.[41,48] This approximation is further supported by the agreement between the theoretical and experimental data for the dependence of the 1s-1s electronic transition on the QD size, in which the QDs have also been treated as spheres.[44,50] The relative increase of the FRET rate and efficiency due to the interaction with the LSPs can be determined by comparison with values calculated from FRET theory,

as previously reported.[20] The theoretical calculations of the FRET rate (given in equation 1) and the FRET efficiency (equation 2) are based on a Förster radius of $R_0 = (3.9 \pm 0.2)\,\mathrm{nm}$ which was determined from the spectral overlap of the donor emission and acceptor absorption and a donor-acceptor centre-to-centre separation of $(23.4 \pm 1.7)\,\mathrm{nm}$.

$$k_{\mathrm{FRET}} = \frac{c_{\mathrm{Acc}} \pi {R_0}^6}{2d^4 \tau_D} \tag{1}$$

$$E_{\mathrm{FRET}} = \frac{1}{1 + \frac{2d^4}{c_{\mathrm{Acc}} \pi {R_0}^6}} \quad . \tag{2}$$

An average FRET rate of $k^{-1}_{FRET-theory} = (500 \pm 200\,\mathrm{ns})^{-1}$, with an average expected FRET efficiency, $E_{FRET-theory} = (0.12 \pm 0.06)\%$, is found for the bilayer structures with no gold nanoparticles and a centre-to-centre donor-acceptor separation of $(23.4 \pm 1.7)\,\mathrm{nm}$, given in Table 1. Variations in the acceptor and donor QD concentration (the latter impacting on the donor lifetimes[48]), result in a spread in the FRET rates calculated for each sample. The theoretically expected FRET rates and efficiencies for each sample are provided in Table S1 in the supporting information along with the details of the parameters relevant for the calculations, such as the QD concentrations.

For the largest gold NP concentration of $c_{Au} = 0.092 \cdot 10^{17}\ \mathrm{m}^{-2}$ a FRET rate of $(2.1 \pm 0.3\,\mathrm{ns})^{-1}$ and a FRET efficiency of $(21 \pm 1)\%$ are determined from the short donor lifetime component, while theory predicts a FRET rate of $(500 \pm 200\,\mathrm{ns})^{-1}$ and a FRET efficiency of $(0.12 \pm 0.06)\%$ for this large donor-acceptor separation. This corresponds to an increase of the FRET rate by a factor of ~200 and a ~150 fold enhancement of the FRET efficiency. Including all the uncertainties on the experimentally measured quantities results in relatively large errors on the calculated FRET rates and efficiencies, but despite

this the enhancements are significant. Furthermore, by calculating back with equation (1) and (2) the apparent Förster radius R_0 in the sandwich structure can be determined from the measured FRET rate and efficiency. The values of R_0 for the sandwich structures with different gold NP concentrations are also included in Table 1. For the highest gold NP concentration investigated, $R_0 = (9.4 \pm 0.4)\,\text{nm}$ is determined, increased by $(240 \pm 20)\%$ over the $(3.9 \pm 0.2)\,\text{nm}$ in a bilayer structure without gold NPs.

Table 1. Different parameters determined for the sandwich structures with varying gold NP concentration (c_{Au}): absolute acceptor PL change (ΔI_{Acc}) [(a)], gold quenched acceptor FRET PL enhancement (ΔI_{Acc-Au}) [(b)], inverse FRET rates measured in the sandwich structure ($k^{-1}_{FRET-LSP}$)[(c)], FRET efficiency ($E_{FRET-LSP}$) determined experimentally for the SP sandwich structure, and Förster radius (R_0) determined from experimental data.

c_{Au} $\left[10^{17}\ \text{m}^{-2}\right]$	ΔI_{Acc} [(a)] [%]	ΔI_{Acc-Au} [(b)] [%]	$k^{-1}_{FRET-LSP}$ [ns]	$E_{FRET-LSP}$ [%]	R_0 [nm]
0			500±200[(c)]	0.12±0.06[(c)]	3.9±0.2
0.026	+ 19	34	-	1.59±0.04	5.9±1.4
0.063	+ 14	49	6±2	8.6±0.2	8.2±0.5
0.086	- 13	24	2.9±0.4	16.9±0.5	9.2±0.4
0.092	- 30	2	2.1±0.3	21±1	9.4±0.4

[(a)] The absolute acceptor PL change ($\Delta I_{Acc} = I_{Acc,Sandwich} / I_{Acc,BL} - 1$) was determined from the integrated acceptor emission in the sandwich structure ($I_{Acc,Sandwich}$) and that of the acceptor-donor bilayer reference ($I_{Acc,BL}$).

[(b)] The gold quenched acceptor PL enhancement ($\Delta I_{Acc-Au} = I_{Acc,Sandwich} / I_{Acc,on\ gold} - 1$) was calculated from the integrated acceptor emission in the sandwich structure ($I_{Acc,Sandwich}$) and that for a corresponding acceptor on gold structure ($I_{Acc,on\ gold}$).

[c] The values given correspond to the average calculated FRET rate, $k^{-1}_{FRET-theory}$, and FRET efficiency, $E_{FRET-theory}$, for a bilayer structure with no gold NP layer and centre-to-centre donor-acceptor separation of $(23.4 \pm 1.7)\,\mathrm{nm}$.

In Table 1 the inverse FRET rate, $k^{-1}_{FRET-LSP}$, the absolute acceptor emission change (compared to the bilayer structure without gold NPs), ΔI_{Acc}, as well as the enhancement of the acceptor emission from the sandwich structure relative to the reference acceptor on gold structure (which exhibits quenched acceptor emission), ΔI_{Acc-Au}, are summarized for the different gold NP concentrations. At the low to intermediate gold NP concentrations an enhancement of the acceptor PL is observed. At the lowest concentration investigated the LSP FRET enhancement of the acceptor PL is greater than the quenching by the gold NPs and an absolute acceptor emission increase of $\Delta I_{Acc} = 19\,\%$ is observed. Although the LSP FRET rate increases with increasing gold NP concentration, the effect of direct PL quenching of the QDs by the gold NPs does too. Consequently, the competition between LSP FRET enhancement of the acceptor PL and direct PL quenching leads to a maximum enhancement of the gold quenched acceptor PL of $\Delta I_{Acc-Au} = 49\,\%$. At the highest gold NP concentrations investigated, where the LSP FRET rate is the highest, the acceptor PL enhancement is low due to the larger direct acceptor emission quenching.

CONCLUSIONS

In conclusion, we have presented further evidence for LSP enhanced FRET in QD sandwich structures with an intermediate gold NP layer and investigated the influence of the gold NP concentration on the signatures of LSP FRET. In the low to intermediate gold NP concentration range an enhancement of the acceptor emission can be observed. An absolute acceptor emission increase of 19% with respect to an acceptor-donor bilayer

structure without gold NPs was realized at the lowest gold concentration investigated, whereas a 49% enhancement of the acceptor emission relative to that quenched by the gold NPs was achieved at a slightly higher gold NP concentration. Even though the highest FRET rates were achieved at the highest gold NP concentrations, the acceptor emission enhancement was reduced for these conditions due to dominating direct quenching by the gold NPs. This clearly shows that careful engineering of the metal NP and QD properties, including the metal NP concentration, is necessary to obtain an optimized LSP FRET effect.

ASSOCIATED CONTENT

Supporting Information. Photoluminescence and absorption spectra for quantum dot and gold nanoparticle monolayers. Quantum dot concentrations as well as fluorescence lifetime analysis data for sandwich and reference structures. This material is available free of charge via the Internet at http://pubs.acs.org.

AUTHOR INFORMATION

Corresponding Author

*Email: bradlel@tcd.ie

† now at Philips Research Laboratories, 5656 AE Eindhoven, The Netherlands

ACKNOWLEDGEMENT

We thank Robert Gunning for the thickness measurements of the polyelectrolyte layers by X-ray diffraction. This work was financially supported by Science Foundation Ireland project 10/IN.1/12975. NG and ALR acknowledge support by a grant from the Germany/Hong Kong Joint Research Scheme sponsored by the Research Grants Council of Hong Kong and the German Academic Exchange Service (Reference No.: G_HK008/10).

REFERENCES

(1) Gersten, J. I.; Nitzan, A. *Chem. Phys. Lett.* **1984**, *104*, 31-37.

(2) Hua, X. M.; Gersten, J. I.; Nitzan, A. *J. Chem. Phys.* **1985**, *83*, 3650-3659.

(3) Govorov, A. O.; Lee, J.; Kotov, N. A. *Phys. Rev. B* **2007**, *76*, 125308.

(4) Förster, T. *Annalen der Physik* **1948**, *2*, 55-75.

(5) Miyawaki, A.; Llopis, J.; Heim, R.; McCaffery, J. M.; Adams, J. A.; Ikura, M.; Tsien, R. Y. *Nature* **1997**, *388*, 882-887.

(6) Medintz, I. L.; Clapp, A. R.; Mattoussi, H.; Goldman, E. R.; Fisher, B.; Mauro, J. M. *Nature Mater.* **2003**, *2*, 630-638.

(7) Willard, D. M.; Mutschler, T.; Yu, M.; Jung, J.; Van Orden, A. *Anal. Bioanal. Chem.* **2006**, *384*, 564-571.

(8) Franzl, T.; Klar, T. A.; Schietinger, S.; Rogach, A. L.; Feldmann, J. *Nano Lett.* **2004**, *4*, 1599-1603.

(9) Lee, J.; Govorov, A. O.; Kotov, N. A. *Nano Lett.* **2005**, *5*, 2063-2069.

(10) Achermann, M.; Petruska, M. A.; Kos, S.; Smith, D. L.; Koleske, D. D.; Klimov, V. I. *Nature* **2004**, *429*, 642-646.

(11) Cicek, N.; Nizamoglu, S.; Ozel, T.; Mutlugun, E.; Karatay, D. U.; Lesnyak, V; Otto, T.; Gaponik, N.; Eychmüller, A.; Demir, H. V. *Appl. Phys. Lett.* **2009**, *94*, 061105.

(12) Chanyawadee, S.; Lagoudakis, P. G.; Harley, R. T.; Charlton, M. D. B.; Talapin, D. V.; Huang, H. W.; Lin, C. H. *Adv. Mater.* **2010**, *22*, 602-606.

(13) Nizamoglu, S.; Sari, E.; Baek, J. H.; Lee, I. H.; Demir, H. V. *New J. Phys.* **2008**, *10*, 123001.

(14) Zhang, J.; Fu, Y.; Lakowicz, J. R. *J. Phys. Chem. C* **2007**, *111*, 50-56.

(15) Lessard-Viger, M.; Rioux, M.; Rainville, L.; Boudreau, D. *Nano Lett.* **2009**, *9*, 3066-3071.

(16) L.-Viger, M.; Brouard, D., Boudreau, D. *J. Phys. Chem. C* **2011**, *115*, 2974-2981.

(17) Komarala, V. K.; Bradley, A. L.; Rakovich, Y. P.; Byrne, S. J.; Gun'ko, Y. K.; Rogach, A. L. *Appl. Phys. Lett.* **2008**, *93*, 123102.

(18) Wang, C. H.; Chen, C. W.; Chen, Y. T.; Wei, C. M.; Chen, Y. F.; Lai, C. W.; Ho, M. L.; Chou, P. T.; Hofmann, M. *Appl. Phys. Lett.* **2010**, *96*, 071906.

(19) Su, X. R.; Zhang, W.; Zhou, L.; Peng, X. N.; Pang, D. W.; Liu, S. D.; Zhou, Z. K.; Wang, Q. Q. *Appl. Phys. Lett.* **2010**, *96*, 043106.

(20) Lunz, M.; Gerard, V. A.; Byrne, S. J.; Gun'ko, Y. P.; Lesnyak, V.; Gaponik, N.; Susha, A. S.; Rogach, A. L.; Bradley, A. L. *Nano Lett.* **2011**, *11*, 3341-3345.

(21) Zhao, L.; Ming, T.; Shao, L.; Chen, H.; Wang, J.; *J. Phys. Chem. C* **2012**, *116*, 8287-8296.

(22) Zhao, X.; Wang, P.; Li, B. *Nanoscale* **2011**, *3*, 3056-3059.

(23) West, R. G.; Sadeghi, S. M. *J. Phys. Chem. C* **2012**, DOI: 10.1021/jp305910j

(24) Anger, P.; Bharadwaj, P.; Novotny, L. *Phys. Rev. Lett.* **2006**, *96*, 113002.

(25) Govorov, A. O.; Bryant, G. W.; Zhang, W.; Skeini, T.; Lee, J.; Kotov, N. A.; Slocik, J. M.; Naik, R. R. *Nano Lett.* **2006**, *6*, 984-994.

(26) Guzatov, D. V.; Vaschenko, S. V.; Stankevich, V. V.; Lunevich, A. Y.; Glukhov, Y. F.; Gaponenko, S. V. *J. Phys. Chem. C*, **2012**, *116*, 10723-10733.

(27) Viste, P.; Plain, J.; Jaffoil, R.; Vial, A.; Adam, P. M.; Royer, P. *ACS Nano* **2010**, *4*, 759-764.

(28) Wargnier, R.; Baranov, A. V.; Maslov, V. G.; Stsiapura, V.; Artemyev, M.; Pluot M.; Sukhanova, A.; Nabiev I. *Nano Lett.* **2004**, *4*, 451-457.

(29) Pons, T.; Medintz, I. L.; Sapsford, K. E.; Higashiya, S.; Grimes, A. F.; English, D. S.; Mattoussi, H. *Nano Lett.* **2007**, *7*, 3157-3164.

(30) Zhang, X.; Marocico, C. A.; Lunz, M.; Gerard, V. A.; Gun'ko, Y. P.; Lesnyak, V.; Gaponik, N.; Susha, A. S.; Rogach A. L.; Bradley, A. L. *ACS Nano* **2012**, *6*, 9283-9290.

(31) Kulakovich, O.; Strekal, N.; Yaroshevich, A.; Maskevich, S.; Gaponenko, S.; Nabiev, I.; Woggon, U.; Artemyev, M. *Nano Lett.* **2002,** *2*, 1449.

(32) Komarala, V. K.; Rakovich, Y. P.; Bradley, A. L.; Byrne, S. J.; Gun'ko, Y. K.; Gaponik, N.; Eychmüller, A. *Appl. Phys. Lett.* **2006,** *89*, 253118.

(33) Lesnyak, V.; Wolf, A.; Dubavik, A. Borchardt, L.; Voitekhovich, S. V.; Gaponik, N.; Kaskel, S.; Eychmüller, A. *J. Am. Chem. Soc.* **2011**, *133*, 13413-13420

(34) Ozel, T.; Nizamoglu, S.; Sefunc, M. A.; Samarskaya, O.; Ozel, I. O.; Mutugun, E.; Lesnyak, V.; Gaponik, N.; Eychmüller, A.; Gaponenko, S. V. *et al. ACS Nano* **2011**, *5*, 1328-1334.

(35) Singh, M. P.; Strouse, G. F. *J. Am. Chem. Soc.* **2010**, *132*, 9383-9391.

(36) Gaponenko, S. V. *Optical properties of semiconductor nanocrystals*; Cambridge University Press: Cambridge, 1998.

(37) Rogach, A. L. *Semiconductor nanocrystals quantum dots: synthesis, assembly, spectroscopy and applications*; Springer: Wien, 2008.

(38) Kagan, C. R.; Murray, C. B.; Bawendi, M. G. *Phys. Rev. B* **1996,** *54*, 8633-8643.

(39) Wuister, S. F.; Koole, R.; Donega, C. D.; Meijerink, A. *J. Phys. Chem. B* **2005,** *109*, 5504-5508.

(40) Kim, D. G.; Okahara, S.; Nakayama, M.; Shim, Y. G. *Phys. Rev. B* **2008,** *78*, 239901.

(41) Lunz, M.; Bradley, A. L.; Gerard, V. A.; Byrne, S. J.; Gun'ko, Y. P.; Lesnyak, V.; Gaponik, N. *Phys. Rev. B* **2011**, *83*, 115423.

(42) Lin, Y. C.; Wang, W. J.; Chung, H. L.; Chou, W. C.; Chen, W. K.; Chang, W. H.; Susha, A. S.; Rogach, A. L. *Appl. Phys. Lett.* **2009**, *95*, 133123.

(43) Rogach, A. L.; Koktysh, D. S.; Harrison, M.; Kotov, N. A. *Chem. Mater.* **2000**, *12*, 1526-1528.

(44) Rogach, A. L.; Franzl, T.; Klar, T. A.; Feldmann, J.; Gaponik, N.; Lesnyak, V.; Shavel, A.; Eychmüller, A.; Rakovich, Y. P.; Donegan, J. F. *J. Phys. Chem. C* **2007**, *111*, 14628-14637.

(45) Gittins, D. I.; Caruso, F. *Angew. Chem. - Int. Ed.* **2001**, *40*, 3001-3004.

(46) Jain, P. K.; Lee, K. S.; El-Sayed, I. H.; El-Sayed, M. A. *J. Phys. Chem. B* **2006**, *110*, 7238-7248.

(47) Amendola, V.; Meneghetti, M. *J. Phys. Chem. C* **2009**, *113*, 4277-4285.

(48) Lunz, M.; Bradley, A. L.; Chen, W.-Y.; Gerard, V. A.; Byrne, S. J.; Gun'ko, Y. P.; Lesnyak, V.; Gaponik, N. *Phys. Rev. B* **2010**, *81*, 205316.

(49) Curuchet, C.; Franceschetti, A.; Zunger, A.; Scholes, G. D. *J. Phys. Chem. C* **2008**, *112*, 13336-13341.

(50) Schooss, D.; Mews, A.; Eychmüller, A.; Weller, H. *Phys. Rev. B* **1994**, *49*, 17072.

Table of Contents Graphic